RSC Advances

ROYAL SOCIETY OF CHEMISTRY

www.rsc.org/advances

Cite this: DOI: 10.1039/c0xx00000x

www.rsc.org/xxxxxx

ARTICLE TYPE

Selective Production of $CuSbS_2$, Cu_3SbS_3, and Cu_3SbS_4 Nanoparticles using a Hot Injection Protocol

Shigeru Ikeda,*[a] Shinji Sogawa,[a] Yuji Tokai,[a] Wilman Septina,[a] Takashi Harada[a] and Michio Matsumura[a]

Received (in XXX, XXX) Xth XXXXXXXXX 20XX, Accepted Xth XXXXXXXXX 20XX
DOI: 10.1039/b000000x

Homogeneous Cu-Sb-S nanocrystals with several compositions can be synthesized in a solution through the hot-injection method. Photoelectrochemical analyses of films of these nanoparticles revealed that these nanoparticles have p-type semiconductive characters.

A ternary Cu-Sb-S system contains several compounds such as $CuSbS_2$ (chalcostibite),[1] $Cu_{12}Sb_4S_{13}$ (tetrahedrite),[2] Cu_3SbS_3 (skinnerite),[3] and Cu_3SbS_4 (famatinite).[2,4] Owing to their differences in crystalline structures and atomic compositions, they would have unique optical and electric properties. Indeed, their measured and calculated optical band gaps (E_gs) are quite different. For instance, E_gs of $CuSbS_2$, Cu_3SbS_3 and Cu_3SbS_4 have been determined to be 1.56 eV, 1.89 eV, and 0.98 eV, respectively.[5] These Cu-Sb-S compounds are regarded as promising sulfide materials for photovoltaic application: they are being considered as alternative absorbers to the chalcopyrite compound of $Cu(In,Ga)(S,Se)_2$ (CIGS) since they are composed of low-toxicity and abundant elements. Specifically, the $CuSbS_2$ compound has been studied widely because of its relatively optimal E_g for sun-light absorption, though there have been few reports showing appreciable solar cell properties[6] due probably to the difficulty in obtaining a dense $CuSbS_2$ film without any shunts. Recently, we have successfully prepared a dense $CuSbS_2$ film by an electrochemical route; preliminary conversion efficiency of the solar cell based on the $CuSbS_2$ film reached 3.12%.[7]

It has been reported by several research groups that ternary and quaternary semiconductor nanoparticles, such as CIGS,[8] $CuInS_2$,[9] and Cu_2ZnSnS_4,[10] were prepared via a precipitation reaction in hot organic solutions as precursors of dense thin film photoabsorbers as well as light-absorbing units without sintering them for sensitized solar cells. Hence, nanoparticles of Cu-Sb-S compounds having different crystalline phases would be promising starting units to fabricate solar cells composed of these new photoabsorbers. However, successful fabrication of Cu-Sb-S nanoparticles is limited to those with $Cu_{12}Sb_4S_{13}$ and Cu_3SbS_4 compositions.[2,4]

The above-described literature studies motivated us to fabricate Cu-Sb-S nanoparticles having other compositions and crystalline phases. In this study, we achieved selective syntheses of $CuSbS_2$ and Cu_3SbS_3 nanoparticles for the first time. Selective formation of Cu_3SbS_4 nanoparticles was also demonstrated. Optical characteristics of these nanoparticles dispersed in a solution and photoelectrochemical (PEC) properties of them immobilized on an electrode substrate by using a layer-by-layer deposition technique were also investigated.

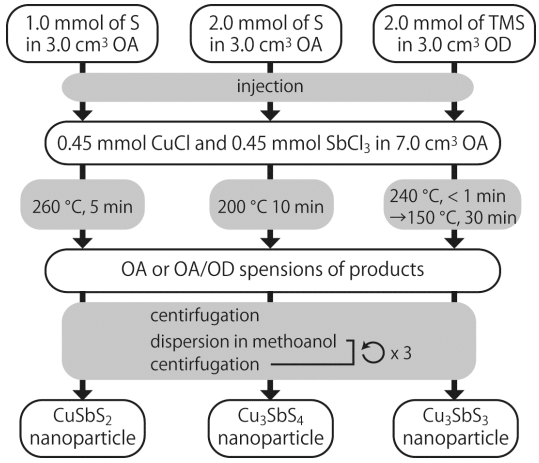

Fig. 1 Flowchart for fabrication of Cu-Sb-S nanoparticles.

Cu-Sb-S nanoparticles were prepared through thermal reactions of metal chloride and elemental sulfur (S) or bis(trimethylsilyl) sulfide (TMS) in a hot solution composed of oleylamine (OA) and 1-octadecene (OD) under an Ar atmosphere. A schematic drawing of the procedures for synthesizing these nanoparticles is shown in Fig. 1. Experimental parameters are also summarized in Table S1. Into an OA solution containing CuCl and $SbCl_3$, a certain amount of S or TMS dissolved in OA or OD was added. Then the mixture was heated for a certain duration. Kinds of sulfur sources, temperatures of the mixtures, and reaction durations varied depending on the target Cu-Sb-S nanoparticles. For the synthesis of $CuSbS_2$ nanoparticles, S dissolved in OA was used and the reaction was performed at 260 °C for 5 min. Cu_3SbS_4 nanoparticles were obtained by injection of S dissolved in OA into the OA solution containing CuCl and $SbCl_3$ at 200 °C; the reaction was continued

at the same temperature for 10 min. Selective formation of Cu_3SbS_3 was achieved by mixing TMS dissolved in OD and the OA solution containing CuCl and $SbCl_3$ at 240 °C for 1 min followed by keeping the mixture at 150 °C for 30 min. After the reactions, large particles were removed from the resulting suspensions by centrifugation. Cu-Sb-S nanoparticles were isolated from the supernatant by precipitation with the addition of methanol.

The XRD pattern of particles synthesized at 260 ˚C for 5 min using a 1:1:2.2 mixture of CuCl, $SbCl_3$ and S exhibited typical diffraction patterns of chalcostibite $CuSbS_2$ without any appreciable reflections of other compounds (Fig. S1a). The XRD pattern of the sample obtained by heating a 1:1:4.4 mixture of CuCl, $SbCl_3$ and S at 200 °C for 10 min showed four broad reflections at 2θ of 28.5°, 32.5°, 47.5°, and 56.5°: these reflections are attributable to (112), (200), (204), and (312) reflections of famatinite Cu3SbS4, respectively (Fig. S1b). A skinnerite Cu_3SbS_3 compound was also obtained by mixing TMS with CuCl and $SbCl_3$ with the Cu:Sb:S molecular ratio of 1:1:4.4 at 240 °C followed by keeping the mixture at 150 °C for 30 min (Fig. S1c).

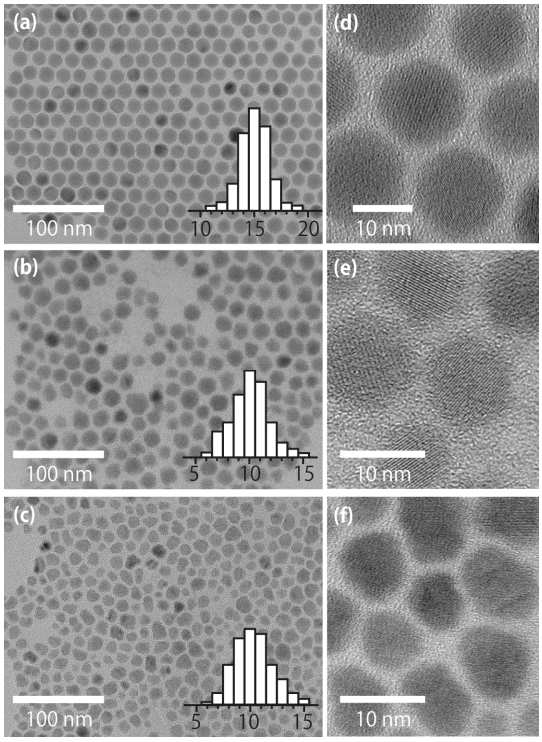

Fig. 2 TEM images of (a,d) $CuSbS_2$, (b,e) Cu_3SbS_4 and (c,f) Cu_3SbS_3 nanoparticles

Fig. 2 shows TEM images of representative Cu-Sb-S nanoparticles. Monodispersed spherical particles were observed in the $CuSbS_2$ nanoparticles, whereas Cu_3SbS_4 and Cu_3SbS_3 samples exhibited polydispersed states having angular morphologies of particles. Based on corresponding size distribution plots of these samples obtained by measuring more than 200 particles (insets of Figs. 2a-c), average diameter (d_{av}) and standard deviation (σ) of these samples were determined; values of d_{av} (σ) were 14.3 nm (1.4 nm) for $CuSbS_2$, 10.5 nm (1.7 nm) for Cu_3SbS_4, and 10.8 nm (1.7 nm) for Cu_3SbS_3. Due to the requirement of a relatively high temperature during the synthesis, $CuSbS_2$ exhibits a relatively large d_{av} value. Reflecting polydispersed states, Cu_3SbS_4 and Cu_3SbS_3 samples have large σ values compared to that of the $CuSbS_2$ sample. As shown in Figs. 2d-f, high-resolution TEM images of these samples revealed that they had a single-crystalline nature: each particle had continuous lattice fringes throughout the particle.

Even by using the same 1:1 mixture of CuCl and $SbCl_3$ solution, we obtained three kinds of nanocrystals with different compositions. In order to examine mechanistic aspects of such selective formation of different nanocrystals, various samples obtained at different temperatures for several reaction durations were analyzed. For example, when the reaction was performed at temperatures less than 200 °C using a solution containing CuCl, $SbCl_3$ and S, a mixture of Cu_2S and Cu_3SbS_4 was initially formed; single-phase Cu_3SbS_4 was obtained by continuing the reaction at a given temperature. These results suggest that formation of Cu_3SbS_4 was through the reaction between initially formed Cu_2S nanocrystals and antimony species in the reaction solution. It should be noted that the formal charge of the antimony component in the Cu_3SbS_4 crystalline is pentavalent (Sb(V)) despite the use of a trivalent antimony (Sb(III)) source. Since the reaction was performed in an Ar atmosphere, oxidation of the Sb(III) component during the formation of Cu_3SbS_4 was likely to be induced by remaining or contaminated oxygen species in the reaction solution.

In separate experiments using mixtures of CuCl/S and $SbCl_3$/S, formation of Cu_2S was confirmed to occur primarily at a relatively low temperature, whereas a binary antimony sulfide (Sb_2S_3) was formed at temperatures higher than 240 °C. Moreover, when the synthesis of Cu-Sb-S nanoparticles was performed at 240 °C, a mixture of Cu_2S, Sb_2S_3, $CuSbS_2$ and Cu_3SbS_3 was obtained. These results indicate that formation of $CuSbS_2$ and Cu_3SbS_3 nanocrystals occurs through the reaction of Cu_2S and Sb_2S_3. This is the reason for the requirement of a relatively high temperature for the formation of single-phase $CuSbS_2$. For the synthesis of Cu_3SbS_3, it should be necessary to avoid formation of Sb(V) because the formal charge of antimony in Cu_3SbS_3 was trivalent. Thus, Sb(III) species in the solution was initially reacted to form Sb_2S_3 at a relatively high temperature in a short period. Then the growth of nanocrystalline Cu_3SbS_3 should be continued at a relatively low temperature (≤ 150 °C) in order to avoid formation of $CuSbS_2$ as well as Cu_3SbS_4. Moreover, for selective synthesis of the Cu_3SbS_3 phase, use of TMS was more suitable than S as a sulfur source: use of S induced contamination of appreciable amounts of Cu_3SbS_4 phase. Relatively high reactivity of TMS with impurity water to produce S^{2-} (or H_2S) would lead to the facilitation of Sb_2S_3 formation with inhibiting oxidation of Sb(III) into Sb(V).

Semi-quantitative analyses of Cu, Sb and S contents of prepared nanoparticles by EDX indicated that compositions of these nanoparticles were almost stoichiometic with the exception of the Cu_3SbS_3 sample that was obviously Cu-poor (Cu/Sb/S = 35/17/48) compared to the stoichiometric one (Cu/Sn/Zn = 43/14/43). The above-discussed formation mechanism of the sample suggests that this deviation is due to the insufficient formation of Cu_2S, leading to remaining appreciable amounts of Sb_2S_3 in the final nanoparticles.

Absorption spectra of Cu-Sb-S nanoparticles uniformly suspended in toluene are given in Fig. S2. The Cu_3SbS_4 sample showed the absorption onset at *ca*. 1330 nm, which is similar to the reported spectrum of Cu_3SbS_4 nanoparticles (Fig. S2b).[2,4] $CuSbS_2$ and Cu_3SbS_3 samples showed absorption onsets at relatively shorter wavelength regions, as shown in Figs. S2a and S2c. It should be noted that all of the spectra have appreciable baseline components, suggesting the presence of tiny amounts of contaminants having relatively narrow band gap energies such as Cu_2S and Cu_3SbS_4 (for $CuSbS_2$ and Cu_3SbS_3), while they were not confirmed by the above XRD analyses. From intersects of the linear portions of the curves with the wavelength axis, E_gs of $CuSbS_2$, Cu_3SbS_4 and Cu_3SbS_3 nanoparticles were estimated to be 1.53 eV, 1.72 eV and 0.93 eV, respectively. Deviations from reported E_gs (see above) are likely to be attributed to inaccuracy in the determination of intersects owing to the presence of baseline components.

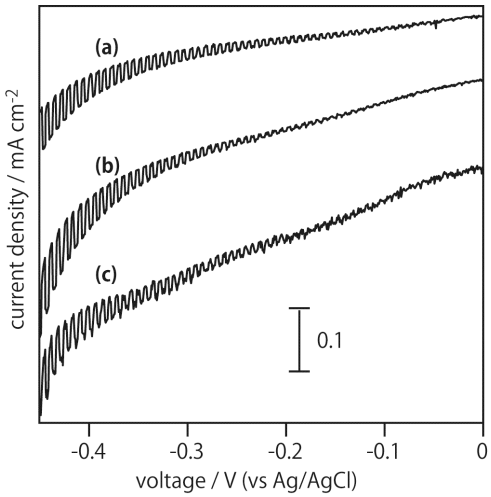

Fig. 3 *LSV* curves of (a) $CuSbS_2$, (b) Cu_3SbS_4 and (c) Cu_3SbS_3 particulate films deposited on an ITO/glass substrate.

In order to determine PEC properties of the Cu-Sb-S nanoparticles, thus-obtained nanoparticles were immobilized on an ITO-coated glass (ITO/glass) substrate. The process for fabrication of these electrodes is described in Supporting Information. Current density-voltage characteristics of particle films were investigated by linear sweep voltammetry (*LSV*) in an aqueous Eu(III) solution at pH adjusted to 4. Fig. 3 shows typical *LSV* plots of the Cu-Sb-S particle films. Since cathodic photocurrents appeared, all of the films prepared in the present study behaved as p-type semiconductor photoelectrodes. As determined by using the lock-in technique, photocurrent onsets of these samples were in the range of -0.1 V to 0.1 V (Fig. S2).11 Although accurate analyses could not be performed because of their weak photoresponses, these results suggest that they have similar energy positions of their valence band edges (E_{VB}s). Due to the appreciable differences of E_gs, conduction band edges (E_{CB}s) of these nanoparticles should be variable. For the application of these p-type compounds to solar cells, therefore, it is required to find suitable n-type compounds to form p-n heterojunctions in view of energy offsets (ΔE_{CB}s) between E_{CB}s of p-type and n-type compounds.[11] In order to study ΔE_{CB}s more accurately, construction of bulk films having sufficient photoresponces by using these nanoparticles as starting materials is now in progress.

Conclusions

$CuSbS_2$, Cu_3SbS_3 and Cu_3SbS_4 nanoparticles with p-type semiconductive properties were successfully synthesized through thermal reactions of metallic ions and S or TMS in high-temperature OA or OA/OD mixed solution. Reaction temperatures higher than 260 °C gave a pure $CuSbS_2$ crystal phase, whereas the Cu_3SbS_4 compound was selectively formed when the reaction temperatures were fixed less than 200 °C. For the synthesis of Cu_3SbS_3 nanoparticle, a two-step heating profile, including generations of both Cu_2S and Sb_2S_3 compounds at 150 °C for a short period followed by reaction between these binary sulfides at 240 °C, was found to be required. We can expect to construct novel light energy conversion systems using these nanoparticles when combined with appropriate n-type compounds.

This work was carried out as part of a program supported by NEDO Japan and a Grant-in-Aid for Scientific Research on Innovative Areas (All Nippon Artificial Photosynthesis Project for Living Earth) from MEXT Japan. Financial support by The Murata Science Foundation is acknowledged. Dr. Takao Sakata (Osaka University) is also acknowledged for their help in TEM measurements.

Notes and references

[a] *Research Center for Solar Energy Chemistry, Osaka University, 1-3 Machikaneyama, Toyonaka, Osaka 560-8531, Japan. Fax: 81 6 6850 6699; Tel: 81 6 6850 6696; E-mail: sikeda@chem.es.osaka-u.ac.jp*

† Electronic Supplementary Information (ESI) available: Experimental details and additional figures. See DOI: 10.1039/b000000x/

1 H. Su, Y. Xie, S. Wan, B. Li and Y. Qian, *Solid State Ionics*, 1999, **123**, 319; Y. Rodriguez-Lazcano, M. T. S. Nair and P. K. Nair, *J. Cryst. Growth*, 2001, **223**, 399; A. Rabhi, M. Kanzari and B. Rezig, *Mater. Lett.*, 2008, **62**, 3576; C. Garza, S. Shaji, A. Arato, E. P. Tijerina, G. A. Castillo, T. K. Das Roy and B. Krishnan, *Sol. Energy Mater. Sol. Cells*, 2011, **95**, 2001; J. T. R. Dufton, A. Walsh, P. M. Panchmatia, L. M. Peter, D. Colombara, and M. Saiful Islam, *Phys. Chem. Chem. Phys.*, 2012, **14**, 7229; D. J. Temple, A. B. Kehoe, J. P. Allen, G. W. Watson and D. O. Scanlon, *J. Phys. Chem. C*, 2012, **116**, 7334.

2 J. van Embden, K. Latham, N. W. Duffy and Y. Tachibana, *J. Am. Chem. Soc.*, 2013, **135**, 11562.

3 D. Chen, G. Shen, K. Tang, X. Jiang, L. Huang, Y. Jin and Y. Qian, *Mater. Res. Bull.*, 2003, **38**, 509; M. X. Wang, G. H. Yue and P. X. Yan, *J. Cryst. Growth*, 2008, **310**, 3062.

4 J. van Embden and Y. Tachibana, *J. Mater. Chem.*, 2012, **22**, 11466.

5 L. Yu , R. S. Kokenyesi , D. A. Keszler and A. Zunger, *Adv. Energy Mater.*, 2013, **3**, 43-48.

6 Y. Rodriguez-Lazcano, M. T. S. Nair and P. K. Nair, *J. Electrochem. Soc.*, 2005, **152**, G635.

7 W. Septina, S. Ikeda, Y. Iga, T. Harada and M. Matsumura, *Thin Solid Films* 2014, **550**, 700.

8 J. Tang, S. Hinds, S. O. Kelley and E. H. Sargent, *Chem. Mater.*, 2008, **20**, 6906; Q. J. Guo, G. M. Ford, R. Agrawal and H. W. Hillhouse, *Prog. Photovolt: Res. Appl.*, 2013, **21**, 64.

9 S. L. Castro, S. G. Bailey, R. P. Raffaelle, K. K. Banger and A. F. Hepp, *J. Phys. Chem. B*, 2004, **108**, 12429; M. G. Panthani, V. Akhavan, B. Goodfellow, J. P. Schmidtke, L. Dunn, A. Dodabalapur, P. F. Barbara and B. A. Korgel, *J. Am. Chem. Soc.*, 2008, **130**, 16770.

10 Q. J. Guo, H. W. Hillhouse and R. Agrawal, *J. Am. Chem. Soc.* 2009, **131**, 11672; S. C. Riha, B. A. Parkinson and A. L. Prieto, *J. Am. Chem. Soc.*, 2009, **131**, 12054; C. Steinhagen, M. G. Panthani, V.

Akhavan, B. Goodfellow, B. Koo and B. A. Korgel, *J. Am. Chem. Soc.* 2009, **131**, 12554; T. Kameyama, T. Osaki, K.-i. Okazaki, T. Shibayama, A. Kudo, S. Kuwabatade and T. Torimoto, *J. Mater. Chem.*, 2010, **20**, 5319; A. Khare, A. W. Wills, L. M. Ammerman, D. J. Norrisz and E. S. Aydil, *Chem. Commun.*, 2011, **47**, 11721; M. Li, W.-H. Zhou, J. Guo, Y.-L. Zhou, Z.-L. Hou, J. Jiao, Z.-J. Zhou, Z.-L. Du and S.-X. Wu, *J. Phys. Chem. C*, 2012, **116**, 26507; G. M. Ford, Q. Guo, R. Agrawal and H. W. Hillhouse, *Chem. Mater.*, 2011, **23**, 2626.

11 R. Klenk, *Thin solid films*, 2001, **387**, 135; M. Turcu and U. Rau, *Thin Solid Films*, 2003, **432**, 158.

A table of contents entry

P-type $CuSbS_2$, Cu_3SbS_4, and Cu_3SbS_3 nanoparticles can be synthesized in a solution through the hot-injection method.